

A novel method for analyzing the global stability of inviscid columnar swirling flow in a finite pipe

S. Wang*

16 July 2007

Abstract

We developed a general strategy to study the stability problem of the inviscid columnar swirling flow in a finite pipe based on the perturbation method of linear operators. By virtue of the columnar base state we were able to derive all the necessary formulas used in perturbation method in a manner of separation of variables. We then conduct a necessary benchmark case study based on the solid body rotation flow. We then applied the general method to the Lamb-Oseen vortex and the q-vortex, and found their approximated growth rate functions. The perturbation method proved effective and robust in application to these vortex flows. We also extended the method, by using the analytic continuation, to find the unstable modes with complex growth rates. This analytic continuation method reflects the global nature of the perturbation method. This study fills a major gap in the study of the global stability for swirling flows, and will have a positive impact on the study of the vortex breakdown phenomenon.

*e-mail: wang@math.auckland.ac.nz

Contents

1	Introduction	3
2	The stability equation for columnar swirling flow	5
3	General approach to columnar swirling flows	7
3.1	The stability equation for a given flow state	7
3.2	Solve the stability problem by using the perturbation method of linear operators	8
3.2.1	The analysis of the operator $T^{(0)}$	10
3.2.2	The analysis of $(T^{(1)}\phi_{o_1,m}^*, \phi_{o_2,n}^*)$ and $(T^{(2)}\phi_{o_1,m}^*, \phi_{o_2,n}^*)$	10
3.2.3	Find the coefficients in the expansion	12
4	A benchmark case study with the solid body rotation flow	13
5	Examples: The Lamb-Oseen vortex and the q-vortex	15
5.1	The Lamb-Oseen vortex with uniform advection	15
5.2	The q-vortex model	20
6	Swirling flow with fixed flowrate at the outlet	21
6.1	General approach	22
6.2	Examples	22
7	Complex growth rate branch	23
8	Conclusions	26
A	The perturbation method	27
A.1	The basic formulas in perturbation method	28
A.2	The derivation of the formulas used in perturbation method	29
B	Evaluation of $I_1(m, n)$ and $I_2(m, n)$	30
	Acknowledgment	31
	References	32

1 Introduction

The study of the stability of an axisymmetric and swirling flow in a pipe goes back to Rayleigh's milestone work [1] in 1916. Rayleigh established a fundamental stability criterion for swirling flows in an infinitely long straight pipe. Rayleigh's criterion states that a columnar swirling flow with a swirl velocity component $V(r)$ and uniform axial velocity components is stable to infinitesimal axisymmetric disturbances if and only if the square of the circulation function, $K = rV$, decreases nowhere as r increases from the center of the pipe to the pipe wall, i.e.:

$$\Phi \equiv \frac{1}{r^3} \frac{d}{dr}(K^2) > 0. \quad (1)$$

Notice that the necessity and sufficiency of (1) for swirling flow being stable are strongly tied with the assumption imposed on the base swirling flow, namely a columnar swirling flow in an infinite pipe. Such flows apparently preserve a translation invariance and therefore admit a Fourier mode analysis without losing any generality. It has since become a common practice in the study of the stability to assume that the flow is uniform in the axial direction. Technically, this often reduces the task to solve an eigenvalue problem with only ordinary differential equations involved. However, in real problem, flows are often seen having significant spatial development and under strong upstream and down stream influence. Applying Rayleigh criterion to these flows could be questionable.

In the study of the vortex breakdown in a finite pipe, the influence of the physical conditions at the pipe inlet and outlet has been studied by Wang and Rusak [2] [3]. It was found that the boundary conditions imposed dramatically alter the stability nature of the swirling flow. In particular, an instability related to the swirl strength was found that can not be explained by the Rayleigh's stability theory. This type of stability has been aptly interpreted by Gallaire and Chomaz [6] as being *global* in nature. Thither, we will use the *global stability* to denote this type of stability.

The global instability which occurs at high swirl is found to be in good correlation with the experimental observations. In experiments (see for example, Garg and Leibovich [4]) it has been observed that the swirl ratio, which is defined as the ratio of the circumferential and axial velocities, can predict the occurrence of vortex breakdown with certain degree of success. Recent experiment of Mattner *et al.* [5] has showed that the occurrence of bubble type vortex breakdown can be predicted by Wang and Rusak's global bifurcation diagram [3].

For further revealing the role of the global stability in the vortex breakdown phenomenon, one must compare the flow transition observed to the prediction of the stability theory. This is particularly important for the study of the vortex breakdown as one notices that several existent vortex breakdown theories, though based on different physical mechanisms have the similar prediction of the swirl for the onset of the breakdown. The mechanism can be clarified by closely inspecting the flow transition and comparing to the theories. This raises the necessity for analyzing the global stability of the flows found in the experiments.

Currently, only one flow model has been thoroughly studied in this aspect, namely, the solid body rotation flow: a column of fluid moving at a constant axial velocity and rotating in a solid body. For this particular model the stability equation could be analytically solved by separating variables, since the axial and radial disturbances in the case could be completely decoupled. However, this method does not fit to solve the stability problems for more realistic swirling flows such as Lamb-Oseen vortex and q-vortex. We will develop a new method in this article to solve the stability problem for an arbitrarily given columnar swirling flow. The method is based on the perturbation theory of the linear operators. The stability problem can be written as an eigenvalue problem of a perturbed linear operator. With this formulation, we may exploit the power of the perturbation theory of linear operators, and solve the stability problem in a general manner.

We first develop the complete techniques for treating the stability problem of the general columnar swirling flows. By virtue of the columnar base state, we show that all the analysis can be done with a manner of separation of variables, a crucial fact to ensure the method effective. We are then able to show a general approach to solve the global stability problem for a given columnar state. The perturbation theory of the linear operators is introduced in the appendix.

We then conduct a *benchmark case study* based on the well studied flow model: *the solid body rotation flow*. Such a benchmark study is necessary. In the perturbation method, one finds and uses a finite terms in a power series to approximate the true function. The effectiveness of the method is dependent on the good behavior of this series. Especially, fast convergence and sufficient large convergence radius are key to the success of the method. Through this benchmark study, we establish the effectiveness and correctness of the method, and learn at the same time the general behaviors of the method.

We then apply the method to two important vortex flows: The Lamb-Oseen vortex and

the q-vortex, and found their approximated growth rate functions. Two types of boundary conditions have been considered, one with non-radial velocity at the outlet, and the other with fixed flowrate at the outlet. The perturbation method proved effective and robust in application to these vortex flows. With low order approximation, of which the computation cost is negligible, a large part of the growth rate function can be accurately found in an algebraic form. The errors of the approximations can be understood by the solid body rotation flow case. In fact, the growth rate curves of various vortex flows have demonstrated a similarity among them. The similarity is of course only qualitatively. Quantitatively, they differ from each other.

We extend the method by using the analytic continuation, and find the unstable modes with complex growth rates. These are oscillating modes, which exist in a specific range of swirl for all columnar swirling flows. A very interesting feature in use of the analytic continuation is as that one does not need to find another expansion for the complex growth rate, instead, one simply make use of real growth rate function, extend it to the complex plane, and thereby find the complex branch. These unstable oscillating modes would generate significant flow dynamics, and are possible related to the observed oscillations of the vortex breakdown bubbles.

Through this study, we establish an effective and useful tool to study the global stability problem for the inviscid columnar swirling flow in a finite pipe. This fills a gap in the study of the dynamics of the swirling flow, and will have a positive impact on the research of the vortex breakdown phenomenon.

2 The stability equation for columnar swirling flow

We consider axisymmetric, incompressible and inviscid flow in a finite length pipe. We use cylindrical coordinates (r, θ, x) , and the velocity components (u, v, w) corresponding to the radial, azimuthal, and axial velocity, respectively. In the dimensionless form, the pipe radius is set as a unit and the pipe length as L , rescaled with respect to the pipe radius. By virtue of the axisymmetry, the stream function $\psi(x, r, t)$ can be defined such that $u = -\psi_x/r$, and $w = \psi_r/r$. Let $y = r^2/2$, in terms of this new variable, $w = \psi_y$, $u = -\frac{\psi_x}{\sqrt{2y}}$ and the reduced form of azimuthal vorticity $\chi = -(\psi_{yy} + \psi_{xx}/2y)$ (the azimuthal vorticity $\eta = \frac{\chi}{r}$).

The Euler equation in terms of ψ , χ and the circulation function K , defined as $K = rv$, can be written in a compact form (see for example Szeri and Holmes [7]):

$$K_t + \{\psi, K\} = 0,$$

$$\chi_t + \{\psi, \chi\} = \frac{1}{4y^2}(K^2)_x, \quad (2)$$

where the brackets $\{f, g\}$ is the canonical Poisson bracket or Jacobian defined as:

$$\{f, g\} = f_y g_x - f_x g_y. \quad (3)$$

For the steady state, $\psi(x, y)$ satisfies the well-known steady Squire-Long equation, which can be derived from equation (2), see Squire [8] and Long [9]:

$$\psi_{yy} + \frac{\psi_{xx}}{2y} = H'(\psi) - \frac{I'(\psi)}{2y}, \quad (4)$$

where $H = p/\rho + (u^2 + v^2 + w^2)/2$ is the total head function (p is pressure and ρ density) $I = K^2/2$ is the extended circulation, both of which are functions of $\psi(x, y)$ only.

Throughout this article, we consider a steady, columnar swirling base flow with the velocity components specified by:

$$(u, v, w) = (0, \omega v_0(y), w_0(y)), \quad (5)$$

where $\omega > 0$ is the swirl parameter. From this velocity profile, one may find $\psi_0(y) = \int_0^y w_0(y) dy$, $\chi_0 = -(\psi_{0yy} + \psi_{0xx}/2y) = -w_{0y}(y)$, $K = \omega K_0(y)$ with $K_0(y) = \sqrt{2y}v_0(y)$ and $I = \omega^2 I_0$ with $I_0 = K_0^2/2$.

In the study of linear stability disturbances of stream function ψ_1 and circulation K_1 are assumed in the forms:

$$\begin{aligned} \psi_1(x, y, t) &= \epsilon \phi(x, y) e^{\sigma t}, \\ K_1(x, y, t) &= \epsilon k(x, y) e^{\sigma t}. \end{aligned} \quad (6)$$

with $\epsilon \ll 1$, where σ is in general a complex number which gives the growth rate. These disturbance terms are superimposed to the base flow state and substituted into the Euler equation (2). By neglecting the second order perturbation terms, one obtains

$$\begin{aligned} &(\phi_{yy} + \frac{\phi_{xx}}{2y} - (H''(\psi_0) - \frac{I''(\psi_0)}{2y})\phi)_{xx} \\ &+ \frac{\sigma \chi_{0y}}{w_0^2} \phi_x + \frac{2\sigma}{w_0} (\phi_{yy} + \frac{\phi_{xx}}{2y})_x + \frac{\sigma^2}{w_0^2} (\phi_{yy} + \frac{\phi_{xx}}{2y}) = 0. \end{aligned} \quad (7)$$

For the detailed derivation of (7) see Wang and Rusak [3]. (7) is the basic stability equation in this study. Notice that this equation can be used for columnar swirling flows with or without the axial shear ($w_0(y)$ may not be constant).

The eigenvalue problem (7) shall be solved subject to a set of boundary conditions. We consider the boundary conditions same as in Wang and Rusak [3]:

$$\begin{aligned}
\phi(x, 0) &= 0, \quad \phi(x, 1/2) = 0, \quad \text{for } 0 \leq x \leq L, \\
\phi(0, y) &= 0, \quad \phi_{xx}(0, y) = 0, \quad k(0, y) = 0, \quad \text{for } 0 \leq y \leq 1/2, \\
\phi_x(L, y) &= 0, \quad \text{for } 0 \leq y \leq 1/2.
\end{aligned} \tag{8}$$

Further more, $k(0, y) = 0$ can be replaced by:

$$\phi_{yyx}(0, y) + \frac{\phi_{xxx}(0, y)}{2y} - \left(H''(\psi_0) - \frac{I''(\psi_0)}{2y} \right) \phi_x(0, y) = 0. \tag{9}$$

These boundary conditions specify a fixed K , χ and w at the inlet and a fixed u at the outlet. We will also consider another set of boundary conditions later on.

3 General approach to columnar swirling flows

In this section we will apply the perturbation method to study the stability equation of the columnar swirling flow. We derive the stability equation for a given columnar swirling flow, and reformulate it as a perturbation problem. We then develop the detailed techniques to solve this perturbation problem. The perturbation method of linear operators is introduced in Appendix A.

3.1 The stability equation for a given flow state

In the stability equation, the term

$$H''(\psi_0) - \frac{I''(\psi_0)}{2y}, \tag{10}$$

shall be determined from the given columnar flow state: $\psi = \psi_0(y)$ and $K = \omega K_0(y)$. One has $I = \omega^2 I_0(y)$, or written as $I = \Omega I_0(y)$ by using a rescaled swirl parameter $\Omega = \omega^2$. We may write (10)

$$H''(\psi_0; \Omega) - \frac{\Omega I_0''(\psi_0)}{2y}, \tag{11}$$

to indicate that $H''(\psi_0; \Omega)$ is dependent on the parameter Ω . From Squire-Long equation (4), one obtains

$$\psi_{0yy} = w_{0y} = H'(\psi_0; \Omega) - \frac{\Omega I_0'(\psi_0)}{2y}. \tag{12}$$

By differentiating (12) with respect to y , one obtains

$$w_{0yy} = H''(\psi_0; \Omega)w_0 - \frac{\Omega I_0''(\psi_0)w_0}{2y} + \frac{\Omega I_0'(\psi_0)}{2y^2}, \quad (13)$$

which gives a explicit formula of (11) in terms of w_0 and I_0 :

$$H''(\psi_0; \Omega) - \frac{\Omega I_0''(\psi_0)}{2y} = \frac{w_{0yy}}{w_0} - \frac{\Omega I_0'(\psi_0)}{2w_0 y^2}. \quad (14)$$

We may now write (7) explicitly in terms of the given columnar state

$$\begin{aligned} & [\phi_{yy} + \frac{\phi_{xx}}{2y} - (\frac{w_{0yy}}{w_0} - \frac{\Omega I_0'(\psi_0)}{2w_0 y^2})\phi]_{xx} \\ & - \frac{\sigma w_{0yy}}{w_0^2}\phi_x + \frac{2\sigma}{w_0}(\phi_{yy} + \frac{\phi_{xx}}{2y})_x + \frac{\sigma^2}{w_0^2}(\phi_{yy} + \frac{\phi_{xx}}{2y}) = 0, \end{aligned} \quad (15)$$

where, one also uses the relation $\chi_{0y} = -w_{0yy}$.

We may define $m(y)$ by

$$m(y) = \frac{2w_0 y^2}{I_0'(\psi_0)} = \frac{2w_0^2 y^2}{(I_0(\psi_0(y)))_y} \quad (16)$$

provided $(I_0(\psi_0(y)))_y$ nowhere vanishes in the interval $(0, \frac{1}{2})$.

Integrating (15) twice along the x -direction by using whichever boundary conditions (8) applicable and multiplying the entire equation with $m(y)$, the stability equation of the general columnar swirling flow is effectively written as a perturbation problem:

$$\begin{aligned} & \underbrace{\int_0^x -m(y)[\frac{2}{w_0}(\phi_{yy} + \frac{\phi_{xx}}{2y}) - \frac{w_{0yy}}{w_0^2}]dx}_{T^{(1)}} + \sigma^2 \underbrace{\int_0^x \int_0^x -\frac{m(y)}{w_0^2}(\phi_{yy} + \frac{\phi_{xx}}{2y})dx dx}_{T^{(2)}} = \underbrace{\Omega\phi}_{T^{(0)}}, \end{aligned} \quad (17)$$

which is subject to the boundary conditions left:

$$\begin{aligned} \phi(x, 0) &= 0, \quad \phi(x, 1/2) = 0, \quad \text{for } 0 \leq x \leq L, \\ \phi(0, y) &= 0, \quad \text{for } 0 \leq y \leq 1/2, \\ \phi_x(L, y) &= 0, \quad \text{for } 0 \leq y \leq 1/2. \end{aligned} \quad (18)$$

3.2 Solve the stability problem by using the perturbation method of linear operators

The stability problem can be written as a perturbed eigenvalue problem of a linear operator in the form:

$$T(\sigma)\phi = \Omega\phi \quad \text{where } T(\sigma) = T^{(0)} + \sigma T^{(1)} + \sigma^2 T^{(2)}. \quad (19)$$

Notice that the growth rate σ appears in (19) as a given perturbation parameters while the swirl parameter Ω is the eigenvalue to be sought.

The key observation of this perturbation problem is that the unperturbed problem

$$T^{(0)}\phi = \Omega\phi \quad (20)$$

can be solved by the method of separation of variables for all columnar state. The eigenvalues of $T^{(0)}$, called as critical swirls, are corresponding to the special flow states where neutral modes exist. At the critical swirl Ω_c , the growth rate $\sigma = 0$, and one seeks the following expansion

$$\Omega = \Omega_c + \sum_{n=1}^{\infty} c_n \sigma^n. \quad (21)$$

In the perturbation theory it can be proved that the formal expansion actually converges to an analytic function in a disc in the complex plane. Technically, all the coefficients in the expansion (21) can be found from the operators $T^{(0)}$, $T^{(1)}$ and $T^{(2)}$ in a systematic way. In Appendix A, we present the perturbation theory and show how to apply it to the stability problem. In particular, explicit formulas for evaluating the coefficients are given. From this appendix, we found the following steps to perform the perturbation method:

1. Find a proper inner product such that the unperturbed operator $T^{(0)}$ is symmetric about this inner product and solve the eigenvalue problem for $T^{(0)}$.
2. Find special inner products involved with the eigenfunctions found in previous step and the operators $T^{(1)}$ and $T^{(2)}$.
3. Evaluate the coefficients in the expansion by using the formulas derived from the perturbation method.

Each of them will be carefully addressed in the following. In the evaluation of the coefficients, we have taken the full advantage of the columnar state and do whatever possible analytic work to simplify the method. At the end, we obtain a set of formulas to perform the perturbation method for stability problem. These formulas are general and ready to be applied to various vortex flows.

3.2.1 The analysis of the operator $T^{(0)}$

Consider the unperturbed eigenvalue problem for $T^{(0)}$

$$-m(y)[(\phi_{yy} + \frac{\phi_{xx}}{2y}) - \frac{w_{0yy}}{w_0}\phi] = \Omega\phi, \quad (22)$$

subject to the boundary conditions (18). The proper Hilbert space of this problem is $L^2_{\frac{1}{m(y)}}(D)$, the $\frac{1}{m(y)}$ weighted square integrable function space on the domain $D = (0, L) \times (0, \frac{1}{2})$ with the inner product defined as:

$$(\phi_1, \phi_2) = \int_D \frac{\phi_1(x, y)\phi_2(x, y)}{m(y)} dx dy. \quad (23)$$

$T^{(0)}$ is a symmetric operator, namely by integrating in parts,

$$\begin{aligned} \int_D \frac{T^{(0)}\phi(x, y)\psi(x, y)}{m(y)} dx dy &= \int_D (\phi_{yy}(x, y) + \frac{\phi_{xx}(x, y)}{2y} - \frac{w_{0yy}}{w_0}\phi)\psi(x, y) dx dy \\ &= \int_D (\psi_{yy}(x, y) + \frac{\psi_{xx}(x, y)}{2y} - \frac{w_{0yy}}{w_0}\psi)\phi(x, y) dx dy = \int_D \frac{T^{(0)}\psi(x, y)\phi(x, y)}{m(y)} dx dy. \end{aligned} \quad (24)$$

The normalized eigenfunctions of (22) denoted by $\phi_{o,n}^*(x, y)$ can be found as

$$\phi_{o,n}^*(x, y) = \sqrt{\frac{2}{L}}\Phi_{o,n}^*(y) \sin\left(\frac{(2n-1)\pi x}{2L}\right), \quad (25)$$

with $\Phi_{o,n}^*(y)$ solving the reduced zeroth order eigenvalue problem

$$\begin{aligned} \Phi_{yy} - \frac{(2n-1)^2\pi^2\Phi}{8L^2y} + \left(\frac{\Omega_{o,n}}{m(y)} - \frac{w_{0yy}}{w_0}\right)\Phi &= 0, \\ \Phi(0) = 0, \Phi\left(\frac{1}{2}\right) &= 0, \end{aligned} \quad (26)$$

and normalized as

$$\left(\int_0^{0.5} \frac{\Phi_{o,n}^{*2}(y)}{m(y)} dy\right)^{\frac{1}{2}} = 1, \quad (27)$$

where, $\Omega_{o,n}$ are eigenvalues with $o = 1, 2, 3, \dots$ and $n = 1, 2, 3, \dots$ in the order $\Omega_{o_1, n_1} \leq \Omega_{o_2, n_2}$ for $o_1 \leq o_2$ and $n_1 \leq n_2$.

3.2.2 The analysis of $(T^{(1)}\phi_{o_1, m}^*, \phi_{o_2, n}^*)$ and $(T^{(2)}\phi_{o_1, m}^*, \phi_{o_2, n}^*)$

Two types of inner products $(T^{(1)}\phi_{o_1, m}^*, \phi_{o_2, n}^*)$ and $(T^{(2)}\phi_{o_1, m}^*, \phi_{o_2, n}^*)$ must be evaluated before further proceeding of the method. According to the definition of $T^{(1)}$ and $T^{(2)}$, one has:

$$\begin{aligned} T^{(1)}\phi_{o,n}^* &= -\int_0^x \frac{2m(y)}{w_0} \left((\phi_{o,n}^*)_{yy} + \frac{(\phi_{o,n}^*)_{xx}}{2y} - \frac{w_{0yy}}{2w_0}\phi_{o,n}^* \right) dx \\ &= \frac{2m(y)}{w_0} \left(\frac{\Omega_{o,n}}{m(y)} - \frac{w_{0yy}}{2w_0} \right) \int_0^x \phi_{o,n}^* dx \\ &= \frac{2m(y)}{w_0} \left(\frac{\Omega_{o,n}}{m(y)} - \frac{w_{0yy}}{2w_0} \right) \Phi_{o,n}^*(y) \int_0^x \sqrt{\frac{2}{L}} \sin\left(\frac{(2n-1)\pi x}{2L}\right) dx. \end{aligned} \quad (28)$$

$$\begin{aligned}
T^{(2)}\phi_{o,n}^* &= -\int_0^x dx \int_0^x \frac{m(y)}{w_0^2} ((\phi_{o,n}^*)_{yy} + \frac{(\phi_{o,n}^*)_{xx}}{2y}) dy \\
&= \frac{m(y)}{w_0^2} \left(\frac{\Omega_{o,n}}{m(y)} - \frac{w_{0yy}}{w_0} \right) \int_0^x dx \int_0^x \phi_{o,n}^* dy \\
&= \frac{m(y)}{w_0^2} \left(\frac{\Omega_{o,n}}{m(y)} - \frac{w_{0yy}}{w_0} \right) \Phi_{o,n}^*(y) \int_0^x dx \int_0^x \sqrt{\frac{2}{L}} \sin\left(\frac{(2n-1)\pi x}{2L}\right) dy. \quad (29)
\end{aligned}$$

We find that $T^{(1)}\phi_{o,n}^*$ and $T^{(2)}\phi_{o,n}^*$ are written in a form with the variables separated. Moreover, the x -dependent functions are but simple trigonometric functions, and can be integrated. By substituting (28) and (29) into $(T^{(1)}\phi_{o_1,m}^*, \phi_{o_2,n}^*)$ and $(T^{(2)}\phi_{o_1,m}^*, \phi_{o_2,n}^*)$, respectively, one finds that the following integrals appear in the expression

$$I_1(m, n) = \int_0^L \sqrt{\frac{2}{L}} \sin\left(\frac{(2n-1)\pi x}{2L}\right) \left(\int_0^x \sqrt{\frac{2}{L}} \sin\left(\frac{(2m-1)\pi x}{2L}\right) dx \right) dx, \quad (30)$$

and

$$I_2(m, n) = \int_0^L \sqrt{\frac{2}{L}} \sin\left(\frac{(2n-1)\pi x}{2L}\right) \left(\int_0^x dx \int_0^x \sqrt{\frac{2}{L}} \sin\left(\frac{(2m-1)\pi x}{2L}\right) dx \right) dx. \quad (31)$$

In Appendix B, these integrals are found, by integration, as:

$$I_1(m, n) = \begin{cases} \frac{8L}{(2m-1)^2\pi^2} & \text{if } n = m, \\ \frac{4L}{(2m-1)\pi^2} \left[\frac{4}{(2n-1)} + \frac{(-1)^{(n+m-1)}-1}{(n+m-1)} + \frac{(-1)^{(n-m)}-1}{(n-m)} \right] & \text{if } n \neq m, \end{cases} \quad (32)$$

and

$$I_2(m, n) = \begin{cases} \frac{4L^2}{\pi^3} \left[\frac{-\pi}{(2m-1)^2} + \frac{4(-1)^{m+1}}{(2m-1)^3} \right] & \text{if } n = m, \\ \frac{(-1)^{n+1}16L^2}{(2n-1)^2(2m-1)\pi^3} & \text{if } n \neq m. \end{cases} \quad (33)$$

These functions reflect the influence of axial disturbance. By using these expressions, one obtains

$$\begin{aligned}
(T^{(1)}\phi_{o_1,m}^*, \phi_{o_2,n}^*) &= I_1(m, n) (\Omega_{o_1,m} (\Phi_{o_1,m}^*, \Phi_{o_2,n}^*)_1 - \frac{1}{2} (\Phi_{o_1,m}^*, \Phi_{o_2,n}^*)_2), \\
(T^{(2)}\phi_{o_1,m}^*, \phi_{o_2,n}^*) &= I_2(m, n) (\Omega_{o_1,m} (\Phi_{o_1,m}^*, \Phi_{o_2,n}^*)_3 - (\Phi_{o_1,m}^*, \Phi_{o_2,n}^*)_4), \quad (34)
\end{aligned}$$

where,

$$\begin{aligned}
(\Phi_{o_1,m}^*, \Phi_{o_2,n}^*)_1 &= \int_0^{\frac{1}{2}} \frac{\Phi_{o_1,m}^* \Phi_{o_2,n}^*}{m(y)w_0} dy, \\
(\Phi_{o_1,m}^*, \Phi_{o_2,n}^*)_2 &= \int_0^{\frac{1}{2}} \frac{w_{0yy}}{w_0^2} \Phi_{o_1,m}^* \Phi_{o_2,n}^* dy, \\
(\Phi_{o_1,m}^*, \Phi_{o_2,n}^*)_3 &= \int_0^{\frac{1}{2}} \frac{\Phi_{o_1,m}^* \Phi_{o_2,n}^*}{m(y)w_0^2} dy, \\
(\Phi_{o_1,m}^*, \Phi_{o_2,n}^*)_4 &= \int_0^{\frac{1}{2}} \frac{w_{0yy}}{w_0^3} \Phi_{o_1,m}^* \Phi_{o_2,n}^* dy. \quad (35)
\end{aligned}$$

It is interesting to see that when the axial shear is not present,

$$\begin{aligned}(\Phi_{o_1,m}^*, \Phi_{o_2,n}^*)_2 &= \int_0^{\frac{1}{2}} \frac{w_{0yy}}{w_0^2} \Phi_{o_1,m}^* \Phi_{o_2,n}^* dy = 0 \\(\Phi_{o_1,m}^*, \Phi_{o_2,n}^*)_4 &= \int_0^{\frac{1}{2}} \frac{w_{0yy}}{w_0^3} \Phi_{o_1,m}^* \Phi_{o_2,n}^* dy = 0.\end{aligned}\quad (36)$$

And (34) reduces to

$$\begin{aligned}(T^{(1)}\phi_{o_1,m}^*, \phi_{o_2,n}^*) &= \Omega_{o_1,m} I_1(m, n) (\Phi_{o_1,m}^*, \Phi_{o_2,n}^*)_1, \\(T^{(2)}\phi_{o_1,m}^*, \phi_{o_2,n}^*) &= \Omega_{o_1,m} I_2(m, n) (\Phi_{o_1,m}^*, \Phi_{o_2,n}^*)_3.\end{aligned}\quad (37)$$

The influence of the axial shear is partially represented by the terms of $(\Phi_{o_1,m}^*, \Phi_{o_2,n}^*)_2$ and $(\Phi_{o_1,m}^*, \Phi_{o_2,n}^*)_4$. Note that the axial shear also affects the reduced zeroth order eigenvalue problem as a term $-\frac{w_{0yy}}{w_0}$ appears in (17).

3.2.3 Find the coefficients in the expansion

With these preparation, we are ready to apply the perturbation method. At each critical swirl $\Omega_{o,m}$, let $\Delta_{o,m}\Omega(\sigma)$ be the swirl increment as a function of σ . The actual swirl can then be written in terms of $\Delta_{o,m}\Omega(\sigma)$ as

$$\Omega = \Omega_{o,m} + \Delta_{o,m}\Omega(\sigma).\quad (38)$$

The perturbation theory of linear operators claims that the function $\Delta_{o,m}\Omega(\sigma)$ is analytic in a complex disc, and has a power series expansion:

$$\Delta_{o,m}\Omega(\sigma) = \Omega_{o,m}^{(1)}\sigma + \Omega_{o,m}^{(2)}\sigma^2 + \Omega_{o,m}^{(3)}\sigma^3 + \dots .\quad (39)$$

The coefficients in the power series are explicitly given by

$$\begin{aligned}\Omega_{o,m}^{(1)} &= (T^{(1)}\phi_{o,m}^*, \phi_{o,m}^*), \\ \Omega_{o,m}^{(2)} &= (T^{(2)}\phi_{o,m}^*, \phi_{o,m}^*) - \sum_{o_1,n:(o_1,n)\neq(o,m)} \frac{(T^{(1)}\phi_{o,m}^*, \phi_{o_1,n}^*)(T^{(1)}\phi_{o_1,n}^*, \phi_{o,m}^*)}{\Omega_{o_1,n} - \Omega_{o,m}}.\end{aligned}\quad (40)$$

In Appendix A one may find the general method to derive $\Omega_{o,m}^{(n)}$, $n = 3, 4$.

We have found that the general columnar swirling flows with or without axial shear are all suitable to be analyzed by the linear operator perturbation method. The key observation is that the unperturbed operator $T^{(0)}$, and its interaction to the perturbed operators $T^{(1)}$ and $T^{(2)}$, can all be analyzed by the method of separation of variable by virtue of the columnar

base state. Notice that the original stability equation can not be analyzed by the method of separation of variables with the only exception of the solid body rotation flow case. The perturbation method actually breaks up the whole problem into sub-problems, each of which can be readily analyzed by the method of separation of variables.

4 A benchmark case study with the solid body rotation flow

The solid body rotation flow is defined as a column of fluid flowing at constant axial velocity $w_0(r) \equiv W_0$, and solid body rotation: $v_0(r) = \omega r$ and $u_0(r) = 0$, where ω is the swirl parameter. For this flow, assuming $W_0 = 1$, the stability equation (7) takes a particular simple form

$$(\phi_{yy} + \frac{\phi_{xx}}{2y} + \frac{\Omega}{2y}\phi)_{xx} + 2\sigma(\phi_{yy} + \frac{\phi_{xx}}{2y})_x + \sigma^2(\phi_{yy} + \frac{\phi_{xx}}{2y}) = 0, \quad (41)$$

where $\Omega = 4\omega^2$ is a rescaled swirl parameter. Carefully examining this equation, one can find that all terms except ϕ_{yy} have a common factor $\frac{1}{2y}$. This makes it possible to be solved by the method of separation of variables. For the detailed analysis, we refer to Wang and Rusak [3] and Gallaire and Chomaz [6]. As a well studied case with an accurate growth rate function available, the solid body rotation flow serves as an ideal vortex model for us to conduct a benchmark case study of the new method, a necessary task for validating the new approach.

By using the perturbation method, the stability equation takes the form

$$\begin{aligned} (\phi_{yy} + \frac{\phi_{xx}}{2y} + \frac{\Omega}{2y}\phi) + \sigma \int_0^x 2(\phi_{yy} + \frac{\phi_{xx}}{2y})dx \\ + \sigma^2 \int_0^x \int_0^x (\phi_{yy} + \frac{\phi_{xx}}{2y})dx dx = 0. \end{aligned} \quad (42)$$

The growth rates of the solid body rotation flow have been computed for a concrete case where pipe length is $L = 10$. We now examine the first and second branch of approximations. Figure 1 shows the results from first order to fourth order approximation. We find from this plot:

1. The first order approximation is good only in a small σ range, about $\sigma < 0.0001$ and the second to 4th order approximations extend this range up to $\sigma = 0.0005$. Note that $\sigma_{max} \approx 0.0008$.
2. The approximation captures some global nature of the growth rate function. For example, in the second branch of approximation the growth rate curve has a branching point at $(\sigma^*, \Omega^*) \approx (0.00024, 14.906)$ where as shown in Gallaire and Chomaz [6] joined with an

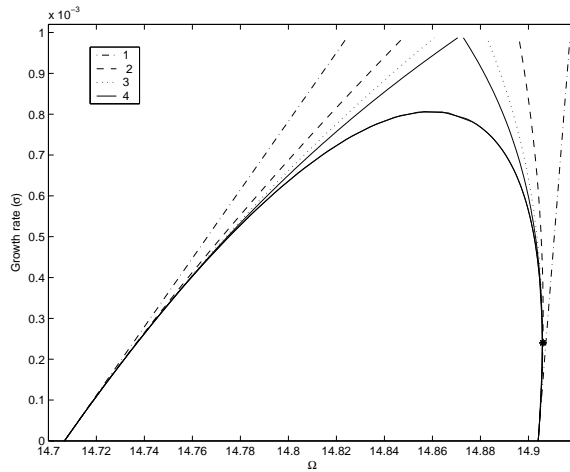


Figure 1: First to 4th order approximations of the growth rate curves between first and second critical swirls. The solid black curve indicates the exact solution. The Asterisk is the branching point.

important complex branch of growth rate curve. This branching point can be found by the approximation with 4th order.

3. The first and second branch of approximations are seen all overshooting the actual growth rate. The approximations are progressively improved as the order goes up. This suggests that the approximation actually gives an upper bound of the real growth rate.
4. Notice that the convergence radius is bounded by σ_{max} , the maximum growth rate in this neighborhood. This is because the function $\Omega(\sigma)$ encounters an infinite derivative and loses its analyticity at σ_{max} . Our computation, however, strongly indicates that the convergence radius is actually σ_{max} .

We now examine the 3rd and 4th branch of approximations. The results are plotted in Figure 2. We find from this plot:

1. The 4th branch of the approximation is similar to the first and second branch. It is again seen that the approximations are straightforward and the obtained value generally overshooting the actual growth rate. A similar branching point $(\sigma^*, \Omega^*) \approx (0.0017, 15.8934)$ is as well captured.
2. The third branch of the approximation has a slightly different behavior. The approximations to the growth rate are seen not any more straightforward. However, the obviously more curved growth rate curve is still well approximated in a slightly smaller range of σ .

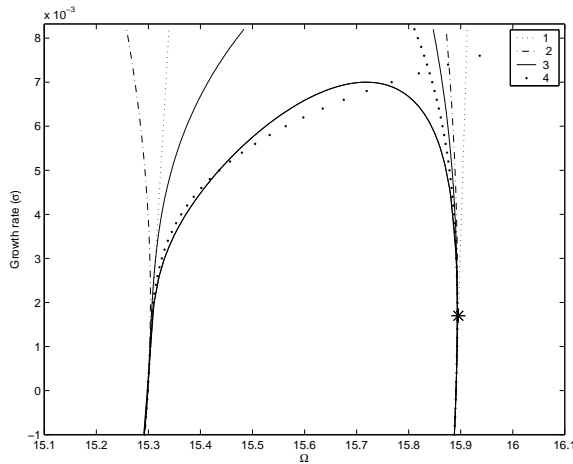


Figure 2: The first to 4th order approximation of the growth rate curves between third and 4th critical swirls. The solid black curve indicates the exact solution. The Asterisk is the branching point.

From this benchmark case study we may conclude that the growth rate of solid body rotation flow can be effectively found by using the linear operator perturbation method. Theoretically, the growth rate can be completely recovered by the power series. Practically the computational cost for finding the coefficients of this series grows dramatically and only low order approximation shall be used. Fortunately, Our computations have demonstrated that with low order such as 4th order approximation, a significant part of growth rate curve covering σ up to $\sigma_{max}/2$ can be found by using the perturbation method and global characteristics of the growth rate function can be captured. Notice that the computational cost is negligible for 4th order approximation.

5 Examples: The Lamb-Oseen vortex and the q-vortex

In this section, the general method will be applied to the Lamb-Oseen vortex. The computed results will be discussed by comparing them to the case of the solid body rotation flow. Computational issues are also addressed whenever necessary. We then apply the method to the q-vortex. Both vortexes are widely used in the study of vortex breakdown phenomena.

5.1 The Lamb-Oseen vortex with uniform advection

The Lamb-Oseen vortex with uniform advection (hither, it will be addressed as Lamb-Oseen vortex.) contains a vortex core at the center in which the flow is similar to the solid

body rotation flow whereas outside this vortex core the flow is close to irrotational flow. The axial velocity of the Lamb-Oseen vortex is uniform and the movement is specified by its axial velocity and its circumferential velocity,

$$\begin{aligned} w_0(r) &= W_0, \\ \omega v_0(r) &= \omega \frac{(1 - e^{-r^2/r_c^2})}{r}, \end{aligned} \quad (43)$$

in which ω is the swirl and r_c is the vortex core. In the study of the stability, the axial velocity can be always rescaled as an unit $W_0 = 1$.

For convenience, let $\beta = 1/r_c^2$, one finds from (43):

$$\begin{aligned} I_0(\psi) &= \frac{1 - 2e^{-2\beta\psi} + e^{-4\beta\psi}}{2}, \\ I_0'(\psi) &= 2\beta e^{-2\beta\psi}(1 - e^{-2\beta\psi}). \end{aligned} \quad (44)$$

From (16), one finds

$$m(y) = \frac{y^2}{\beta(1 - e^{-2\beta y})e^{-2\beta y}}. \quad (45)$$

The stability equation is formulated as the following perturbation problem:

$$\begin{aligned} &\underbrace{-m(y)(\phi_{yy} + \frac{\phi_{xx}}{2y})}_{T^{(0)}} + \sigma \underbrace{\int_0^x [-2m(y)(\phi_{yy} + \frac{\phi_{xx}}{2y})] dx}_{T^{(1)}} \\ &+ \sigma^2 \underbrace{\int_0^x \int_0^x [-m(y)(\phi_{yy} + \frac{\phi_{xx}}{2y})] dx dx}_{T^{(2)}} = \Omega\phi, \end{aligned} \quad (46)$$

subject to the boundary conditions (18).

The reduced zeroth eigenvalue problem of $T^{(0)}$ becomes

$$\begin{aligned} \Phi_{yy}(y) - \frac{(2n-1)^2\pi^2\Phi(y)}{8L^2y} + \frac{\Omega\beta(1 - e^{-2\beta y})e^{-2\beta y}}{y^2}\Phi(y) &= 0, \\ \Phi(0) = 0, \quad \Phi(1/2) &= 0. \end{aligned} \quad (47)$$

The ordinary differential equation (47) have been numerically solved by Matlab standard solver.

For the case β equals 4.0 and L equals 6.0 one finds the first 4 $\Omega_{1,n}$ (see Table 1):

In this case, since the axial shear does not present, we shall use (37) for calculating $(T^{(1)}\phi_{o_1,m}^*, \phi_{o_2,n}^*)$, and $(T^{(2)}\phi_{o_1,m}^*, \phi_{o_2,n}^*)$. In the actual evaluation of the above formulas, because of frequent use of the inner products $(\Phi_{o_1,m}^*, \Phi_{o_2,n}^*)_1$ and $(\Phi_{o_1,m}^*, \Phi_{o_2,n}^*)_3$, they shall be calculated once only at the beginning of the computation and the result will be recalled promptly.

Table 1: Value of $\Omega_{1,n}$ for $n = 1, 2, 3, 4$.

	n = 1	n = 2	n = 3	n = 4
$\Omega_{1,n}$	0.7824	0.8055	0.8509	0.9171

We are now at a stage to calculate the coefficients $\Omega_{o,m}^{(i)}$ in the expansion (39). The computation is based on the case: $\beta = 4$ and $L = 6$. We use the explicit formulas of $(T^{(1)}\phi_{o_1,m}^*, \phi_{o_2,n}^*)$ and $(T^{(2)}\phi_{o_1,m}^*, \phi_{o_2,n}^*)$ found previously. We found that the summation index $n = 20$ is sufficiently large for obtaining an accurate coefficient. For the summation index o , our computation demonstrated that the contribution to the growth rate is dominant by $o = 1$. See Table 2 for the computation results of $\Omega_{1,m}^{(2)}$ for the choice of summation index o up to 1, 2, 3, respectively. We find from this table that a choice of summation index up to $o = 3$ is sufficient for obtaining

Table 2: Value of $\Omega_{1,m}^{(2)}$ calculated with summation index o up to $o = 1, 2, 3$.

o	$m = 1$	$m = 2$	$m = 3$	$m = 4$
1	214.6997	-192.8153	-10.9528	-5.8240
2	214.7012	-192.8136	-10.9516	-5.8218
3	214.7014	-192.8134	-10.9514	-5.8216

an accurate result. If the computational cost is a real concern, the computation for $o = 2, 3$ can be also dropped.

Table 3 shows the calculated results of $\Omega_{1,m}^{(k)}$. The computation is based on the summation terms up to $n = 20$ and $o = 3$.

Table 3: Value of $\Omega_{1,m}^{(k)}$ calculated for $m = 1, 2, 3, 4$ and $k = 1, 2, 3, 4$.

	$m = 1$	$m = 2$	$m = 3$	$m = 4$
$\Omega_{1,m}^{(1)}$	3.8049	0.43526	0.16553	0.091023
$\Omega_{1,m}^{(2)}$	214.70	-192.81	-10.951	-5.8216
$\Omega_{1,m}^{(3)}$	1.0335×10^5	-0.25513×10^5	1.2545×10^3	0.969813×10^2
$\Omega_{1,m}^{(4)}$	6.7487×10^6	-6.8683×10^6	1.0525×10^5	-6.4643×10^3

Figure 3 shows the first and second branches of the growth rate curves based on the coefficients shown above. The approximations from the first to the 4th order are similar to

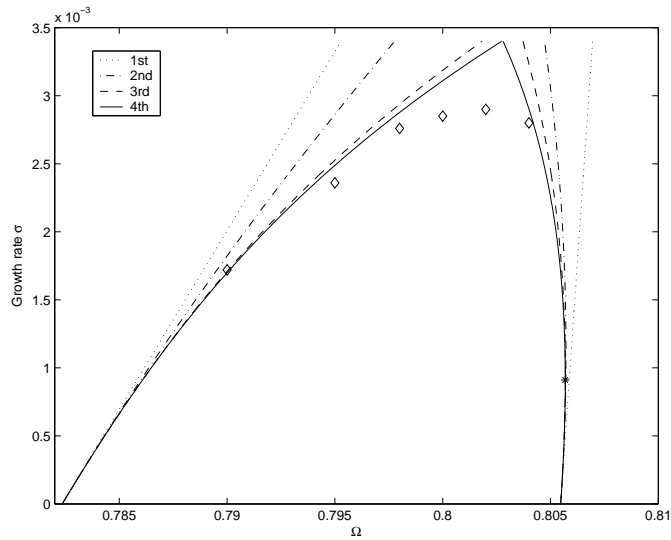


Figure 3: Growth rate σ of the Lamb-Oseen vortex with first to 4th order approximation. The diamonds are result of numerical simulation. The Asterisk is the branching point.

what has been found in the case of the solid body rotation flow. We expect that the accuracy of the approximation shall be also similar. In light of the benchmark case study, we may make the following observations for the results obtained.

1. The first order approximation is good only in a small σ range, about $\sigma = 0.0005$ and the second to 4th order approximations extend this range up to $\sigma = 0.0016$ where the third and 4th order approximations are departing from each other. Note that $\sigma_{max} < 0.0034$, where σ_{max} is the maximum growth rate between the first and second critical swirls.
2. The approximation is global in nature. This can be clearly seen from the second branch of approximation. The growth rate has a branching point at $(\sigma^*, \Omega^*) \approx (9.1 \times 10^{-4}, 0.8057)$ where a complex branch of growth rate curve emanates. This branching point are well captured by the 4th order approximation.
3. The approximations are progressively improved as the order goes up in the first and second branch of approximations. It suggests that the approximation is overshooting the actual growth rate and thus gives an upper bound of the real growth rate.

To confirm the above statements, we have done numerical simulations of the linearized equations of (2). Starting from a given but rather arbitrary initial disturbance, the flow eventually

evolves into a flow state corresponding to the unstable mode with the largest growth rate. As in this case, only one unstable mode exists and its growth rate can then be found in terms of this long time behavior. The second order central difference scheme is used in spatial discretization and the time evolution is integrated by using 4th order Rungs-Kutta method. The simulated growth rates are plotted in the same figure with diamonds. The relation between the actual growth rate and the approximation is indeed very similar to the solid body rotation flow case.

Figure 4 shows the results of the third and the 4th branches of the growth rate based on the coefficients shown above. We find from this plot:

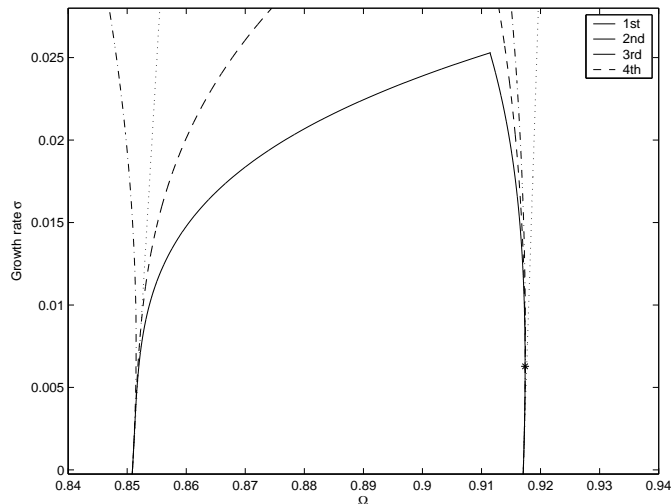


Figure 4: Growth rate σ of the Lamb-Oseen vortex with first to 4th order approximation. The Asterisk is the branching point.

1. The 4th branch of the approximation is similar to the first and second branch. It is again seen that the approximation is straightforward and the obtained value is believed to be overshooting the actual growth rate and thus gives a useful up bound in the range. A similar branching point $(\sigma^*, \Omega^*) \approx (0.0063, 0.9174)$ is as well captured.
2. The third branch of the approximation has a slightly different behavior similar to the solid body rotation case.

Overall, we found that the approximated growth rates are similar to the solid body rotation case. The errors of the approximations are expected to be at the same magnitude as in the solid body rotation flow.

5.2 The q-vortex model

The q-vortex has a circumferential velocity profile same as Lamb-Oseen vortex but allows a non-uniform axial velocity distribution:

$$\begin{aligned} w_0(r) &= W_0 + a_0 e^{-r^2}, \\ \omega v_0(r) &= \omega \frac{(1 - e^{-r^2/r_c^2})}{r}, \end{aligned} \quad (48)$$

where $W_0 > 0$ is a constant giving a uniform axial advection and a_0 a parameter to determine the nature of the axial velocity profile: $a_0 < 0$ corresponds to a wake-like axial velocity profile and $a_0 > 0$, a jet-like.

From (48), we may derive

$$\begin{aligned} I_0(\psi_0(y)) &= \frac{1 - 2e^{-2\beta y} + e^{-4\beta y}}{2}, \\ (I_0(\psi_0(y)))_y &= 2\beta e^{-2\beta y}(1 - e^{-2\beta y}), \end{aligned} \quad (49)$$

where, $\beta = 1/r_c^2$. According to (16), we may find

$$m(y) = \frac{y^2(W_0 + a_0 e^{-r^2})^2}{\beta(1 - e^{-2\beta y})e^{-2\beta y}}. \quad (50)$$

The stability equation of the q-vortex is found as a perturbation problem:

$$\begin{aligned} &\overbrace{[-m(y)(\phi_{yy} + \frac{\phi_{xx}}{2y} - \frac{4a_0 e^{-2y}}{W_0 + a_0 e^{-2y}}\phi)]}^{T^{(0)}} \\ + \sigma \int_0^x &\underbrace{-m(y)[\frac{2}{W_0 + a_0 e^{-2y}}(\phi_{yy} + \frac{\phi_{xx}}{2y}) - \frac{4a_0 e^{-2y}}{(W_0 + a_0 e^{-2y})^2}\phi]}_{T^{(1)}} dx \\ &+ \sigma^2 \int_0^x \int_0^x \underbrace{\frac{-m(y)}{(W_0 + a_0 e^{-2y})^2}[(\phi_{yy} + \frac{\phi_{xx}}{2y})]}_{T^{(2)}} = \Omega \phi. \end{aligned} \quad (51)$$

The reduced zeroth order eigenvalue problem of $T^{(0)}$ (51) becomes

$$\begin{aligned} \Phi_{yy} - \frac{(2n-1)^2 \pi^2 \Phi(y)}{8L^2 y} + \left(\frac{\Omega}{m(y)} - \frac{4a_0 e^{-2y}}{W_0 + a_0 e^{-2y}} \right) \Phi &= 0, \\ \Phi(0) = 0, \Phi(0.5) &= 0. \end{aligned} \quad (52)$$

The weighted inner products are found as

$$(\Phi_{o_1, m}^*, \Phi_{o_2, n}^*)_1 = \int_0^{\frac{1}{2}} \frac{\Phi_{o_1, m}^* \Phi_{o_2, n}^*}{m(y)(W_0 + a_0 e^{-2y})} dy,$$

$$\begin{aligned}
(\Phi_{o_1,m}^*, \Phi_{o_2,n}^*)_2 &= \int_0^{\frac{1}{2}} \frac{4a_0 e^{-2y}}{(W_0 + a_0 e^{-2y})^2} \Phi_{o_1,m}^* \Phi_{o_2,n}^* dy, \\
(\Phi_{o_1,m}^*, \Phi_{o_2,n}^*)_3 &= \int_0^{\frac{1}{2}} \frac{\Phi_{o_1,m}^* \Phi_{o_2,n}^*}{m(y)(W_0 + a_0 e^{-2y})^2} dy, \\
(\Phi_{o_1,m}^*, \Phi_{o_2,n}^*)_4 &= \int_0^{\frac{1}{2}} \frac{4a_0 e^{-2y}}{(W_0 + a_0 e^{-2y})^3} \Phi_{o_1,m}^* \Phi_{o_2,n}^* dy.
\end{aligned} \tag{53}$$

These are explicit formulas used in the computation of the perturbation method. For the cases $\beta = 4$, $W_0 = 1$, $a_0 = \pm 0.2$ and $L = 6$ we find the 4th order approximations, and the results are plotted in Figure 5.

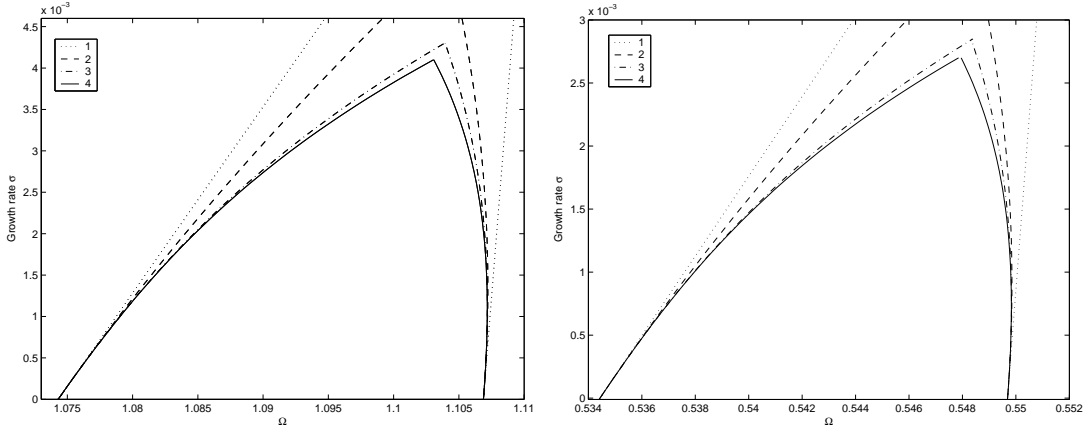


Figure 5: Growth rate σ of the q vortex with first to 4th order approximation. The left plot: $W_0 = 1$ and $a_0 = 0.2$; The right plot: $W_0 = 1$ and $a_0 = -0.2$.

6 Swirling flow with fixed flowrate at the outlet

We address the stability problem with changing the outlet boundary condition to $\psi(t, L) = 0$, which corresponds to the physical setting: a fixed flowrate at the discharge. We consider two type of vortexes: solid body rotation flow as a benchmark case, and the Lamb-Oseen vortex. The results obtained are important for the study of the physical mechanism of the swirling flow in a finite pipe. It can be shown that the energy transfer mechanism of this boundary setting is simpler than the boundary condition (8).

6.1 General approach

The general method introduced in section 2 can be modified to treat this type of boundary conditions. We follow all the steps up to (24), and change (25) to

$$\phi_{o,n}^*(x, y) = \sqrt{\frac{2}{L}} \Phi_{o,n}^*(y) \sin\left(\frac{n\pi x}{L}\right), \quad (54)$$

with $\Phi_{o,n}^*(y)$ solving the reduced zeroth order eigenvalue problem

$$\begin{aligned} \Phi_{yy} - \frac{n^2\pi^2\Phi}{2L^2y} + \left(\frac{\Omega_{o,n}}{m(y)} - \frac{w_{0yy}}{w_0}\right)\Phi &= 0, \\ \Phi(0) = 0, \Phi\left(\frac{1}{2}\right) &= 0, \end{aligned} \quad (55)$$

and normalized according to (27). This change is due to the fact that the x -direction eigenfunction $\sin\left(\frac{(2n-1)\pi x}{2L}\right)$ is now replaced by $\sin\left(\frac{n\pi x}{2L}\right)$,

We then derive explicit expressions of

$$(T^{(1)}\phi_{o_1,m}^*, \phi_{o_2,n}^*) \text{ and } (T^{(2)}\phi_{o_1,m}^*, \phi_{o_2,n}^*), \quad (56)$$

in terms of the eigenfunctions (54). In a similar manner, the following functions can be derived to replace (32) and (33):

$$I_1(m, n) = \begin{cases} \frac{4L}{m^2\pi^2}(1 - (-1)^n), & \text{if } n = m, \\ \frac{4L}{m\pi^2} \left[\frac{1 - (-1)^n}{n} + \frac{(-1)^{(n+m)} - 1}{2(n+m)} + \frac{(-1)^{(n-m)} - 1}{2(n-m)} \right] & \text{if } n \neq m, \end{cases} \quad (57)$$

and

$$I_2(m, n) = \begin{cases} -\frac{L^2}{m^2\pi^2}(1 + (-1)^n \frac{2}{\pi}), & \text{if } n = m, \\ (-1)^{n+1} \frac{2L^2}{mn\pi^3} & \text{if } n \neq m. \end{cases} \quad (58)$$

One thus obtains

$$\begin{aligned} (T^{(1)}\phi_{o_1,m}^*, \phi_{o_2,n}^*) &= I_1(m, n)(\Omega_{o_1,m}(\Phi_{o_1,m}^*, \Phi_{o_2,n}^*)_1 - \frac{1}{2}(\Phi_{o_1,m}^*, \Phi_{o_2,n}^*)_2), \\ (T^{(2)}\phi_{o_1,m}^*, \phi_{o_2,n}^*) &= I_2(m, n)(\Omega_{o_1,m}(\Phi_{o_1,m}^*, \Phi_{o_2,n}^*)_3 - (\Phi_{o_1,m}^*, \Phi_{o_2,n}^*)_4). \end{aligned} \quad (59)$$

A noticeable fact is $I_1(m, m) = 0$ for m even, and thus $\Omega_{o,m}^{(1)} = 0$.

6.2 Examples

We apply the method to the solid body rotation flow with pipe length $L = 10$. The first to 4th order approximations and the comparison to the exact growth rate are plotted in Figure

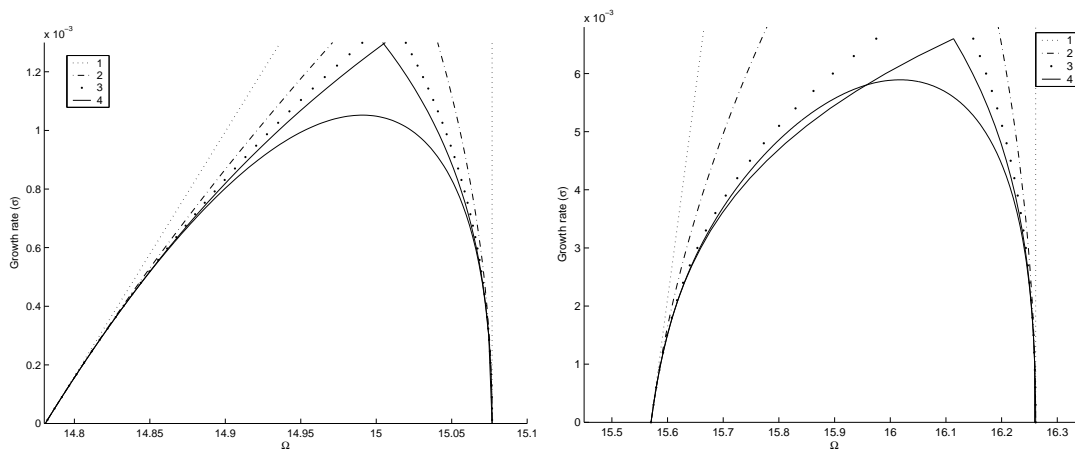


Figure 6: Growth rate σ of the solid body rotation flow with fixed outlet flow. The first to 4th order approximations. The left plot: First and second branch; The right plot: 3rd and 4th branch.

6. We find from this plot that the overall behavior of the approximations is very similar to the case with boundary conditions (8).

We also apply the method to the Lamb-Oseen vortex with the case: $\beta = 4$ and $L = 6$. The first to 4th order approximations are plotted in Figure 7. The growth rate curve again resembles to the solid body rotation flow.

7 Complex growth rate branch

It has been found in Gallaire and Chomaz [6] and Gallaire, Chomaz and Huerre [11] that, besides the real growth rate branch, there exist complex growth rate branches for the solid body rotation flow. The complex growth rates are found to be complex conjugates. The modes associated with the complex growth rate are unstable and oscillating. One would expect that similar complex branches should exist for general columnar swirling flows. The question is how to find them.

The perturbation method discussed here is a global method, in the sense that the analyticity of the function $\Omega(\sigma)$ is a established fact and the power series obtained by the perturbation method is convergent in the complex plane up to the nearest non-analytic point. Although it has not been mathematically proved that the convergence radius is exactly equal to σ_{max} , all computational results indicate that this is the case. In the following, we will make use of this

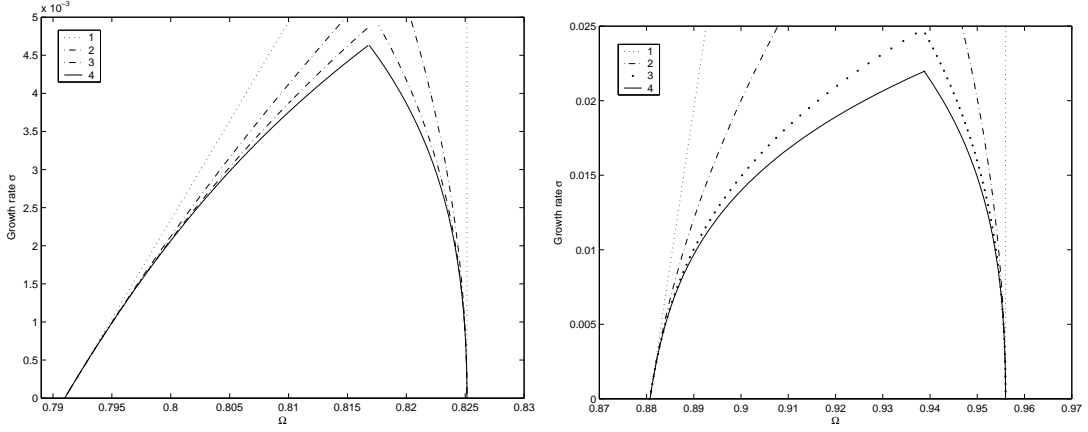


Figure 7: Growth rate σ of the Lamb-Oseen vortex with fixed outlet flow. The first to 4th order approximations. The left plot: first and second branch; The right plot: 3rd and 4th branch.

analyticity and extend the relation between Ω and σ to the complex domain. The analytic continuation of the approximated polynomial will lead to the complex growth rate branch.

We consider at first the case of the solid body rotation flow with the fixed flowrate at the outlet. We found the second branch of approximation as

$$\Delta_{1,2}\Omega(\sigma) \approx -2.1356 \times 10^4 \sigma^2 - 9.6514 \times 10^6 \sigma^3 - 5.3268 \times 10^9 \sigma^4, \quad (60)$$

and the coefficient of σ vanishes and all the other coefficients are negative. Therefore, the swirl increment $\Delta_{1,2}\Omega$ is always negative for real σ . However, if we extend the function $\Delta_{1,2}\Omega(\sigma)$ to the complex plane, we may find a complex growth rate σ which gives rise a positive swirl increment $\Delta_{1,2}\Omega(\sigma) > 0$. The growth rate function can be extended to the swirl above the critical swirl $\Omega_{1,2}$.

To proceed, we need only to seek a complex σ to solve (60) for a given $\Omega > \Omega_{1,2}$. The result is shown in Figure 8. The exact growth rate function is plotted in this figure for comparison. It is found that the complex branch is well approximated in this neighborhood. Notice that the approximation worsens as the norm of the complex growth rate σ is close to σ_{max} (where $\Omega \approx 15.1$). This again indicates that the actual convergence radius of the power series is σ_{max} .

Applying this method to the Lamb-Oseen vortex with the same boundary conditions generates the complex branch for $\Omega > \Omega_{1,2}$. This complex branch is shown in Figure9. It is found from this plot that the curve of the imaginary part of the complex growth rate rises consider-

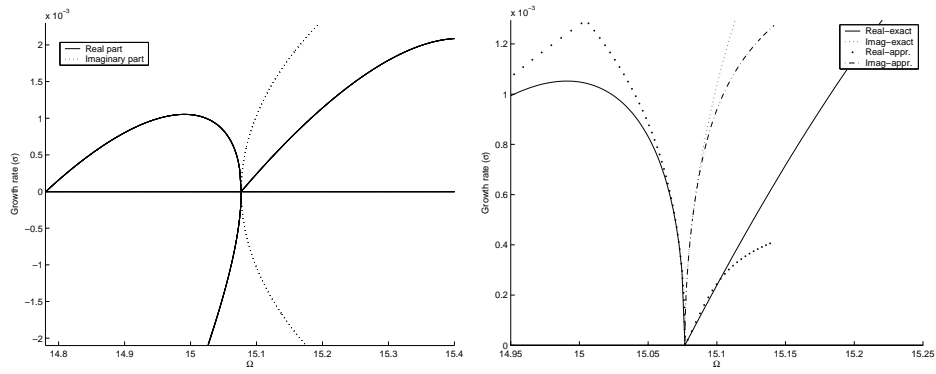


Figure 8: The complex growth rate σ of the solid body rotation flow with fixed outlet flow. The left plot: the exact growth rate; The right plot: comparison to the 4th order approximation.

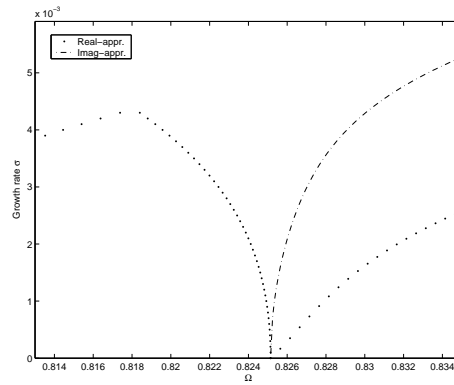


Figure 9: The 4th order approximation of the complex growth rate σ of the Lamb-Oseen vortex with fixed outlet flow .

ably slower than for the case of the solid body rotation flow, and the norm of the growth rate σ reaches the level of σ_{max} at swirl level approximately $\Omega = 0.828$. The approximation of the complex branch is expected to be good up to $\Omega = 0.828$.

8 Conclusions

We have successfully developed a method to solve the global stability problem for general columnar inviscid swirling flows in a finite pipe, and applied the method to various vortex flows. This development fills a gap in the study of the dynamics of the swirling flows. Before this study, only for one single flow, the solid body rotation flow, the global stability has been analyzed. This has been a bottleneck in the study of the dynamics of the swirling flows in a finite pipe for a long time. The research scope has been unavoidably confined in this particular flow. Now, more realistic vortex flows such as Lamb-Oseen vortex and q-vortex can all be analyzed by this method. This certainly opens new opportunities for us to explore the dynamics of swirling flows.

In the context of the vortex breakdown, the global stability has an important role. In the past, the research has been focused on the solid body rotation flow and very interesting physics has been found based on this flow model. The energy transfer mechanism for the solid body rotation flow in a finite pipe found by Gallaire and Chomaz [6] is an interesting and important result. They found that the stability of the solid body rotation flow is solely dependent on the net gain of energy at the boundaries. The vortex core serves only as a neutral waveguide. To extend their result to general swirling flows, one must first solve the stability equation, and find the associated eigenmode. This “need” has originally motivated this research. As a reward, we are now able to conduct a revealing analysis of the energy transfer mechanism for general swirling flows. We have found that in general swirling flows, the energy transfer takes place actively at the boundaries and inside the flow. The work will be reported in a separated paper.

As has been shown, the method developed in this article furnishes a powerful tool for studying the complicated dynamical behaviors of swirling flows in a finite pipe. It greatly expands the scope of the research. Instead of the solid body rotation flow, one may now consider more realistic vortex flow models and study their stability characters and the relevant dynamical behaviors. In the author’s view, the study of the global stability of swirling flows

is still in its early stage. The complicated dynamics of the swirling flows can be related to the global stability in many ways, and is yet to be explored. Although, this article is mainly about development of a effective method, we have yet found many interesting stability results for various vortex flows of which some are worthy to be further studied. We list the following problems and believe that they deserve further attentions.

1. We have found the oscillating unstable modes in certain range of the swirl. We would ask the question of the global dynamical behavior of the flow, such as whether or not a limit cycle would be formed or more complicated dynamics such as chaotic motion would occur.
2. We have found the approximated growth rate function for the Lamb-Oseen vortex and the q-vortex. These flows are known to be stable according to the Rayleigh's criterion. We would want to know the stability characteristic of the swirling flows that are unstable according to the Rayleigh's criterion.
3. We would have to consider a non-columnar swirling flow as the base flow in the case that the physical mechanism is essentially related to the axial non-uniformity of the flow. It is therefore a necessary task to extend the perturbation method to the non-columnar flow.

One may have to make necessary extension of the methods and the results in this article to pursuit these questions.

A The perturbation method

We introduce the perturbation method of the linear operators in this section. We do not intend to cover the general perturbation method, which could become very complicated technically. We recommend Kato [10] for further reading, which is our general reference. In the following, we introduce the basic formulas in the perturbation method, and we restrict our attention to the case where the unperturbed operator $T^{(0)}$ is a selfadjoint operator and the spectrum of $T^{(0)}$ is discrete and simple. This makes the description of the method much more concisely, yet being sufficient for the application in the stability problem.

A.1 The basic formulas in perturbation method

Consider the linear operator $T(\sigma)$ with the form:

$$T(\sigma) = T^{(0)} + \sigma T^{(1)} + \sigma^2 T^{(2)}, \quad (61)$$

in which $T^{(0)}$ is assumed as an unbounded selfadjoint linear operator with a densely defined domain in a Hilbert space, \mathbf{H} and $T^{(1)}$ and $T^{(2)}$ are assumed linear operators relatively bounded by $T^{(0)}$, that is there exist constants a and b such that:

$$\max(\|T^{(1)}u\|, \|T^{(2)}u\|) \leq a\|u\| + b\|T^{(0)}u\| \quad (62)$$

on the domain. Under these assumption, $T(\sigma)$ is proved in Kato [10], a homomorphic function of σ .

Further more, we assume that the spectrum of $T^{(0)}$ is discrete and simple, denoted by $\lambda_0, \lambda_1, \lambda_2, \dots$, with the corresponding orthonormal eigenvectors $\{e_0, e_1, e_2, \dots\}$ (The eigenvalues are aptly denoted by λ rather than the swirl parameter Ω for avoiding possible confusion):

$$T^{(0)}e_0 = \lambda_0 e_0 \quad (63)$$

$$T^{(0)}e_i = \lambda_i e_i, \quad i = 1, 2, \dots$$

We single out the eigenvalue λ_0 here with which we are going to consider the perturbation problem: How does this eigenvalue change if the perturbed term $\sigma T^{(1)} + \sigma^2 T^{(2)}$ is present? We shall denote the perturbed eigenvalue as $\lambda(\sigma)$ to indicate the dependence. From the perturbation theory, we know that, in general, the eigenvalue $\lambda(\sigma)$ is an analytic function of σ in a neighborhood of $\sigma = 0$, and thus $\lambda(\sigma)$ admits a power series expansion in the neighborhood:

$$\lambda(\sigma) = \lambda_0 + \sum_{n=1}^{\infty} \lambda^{(n)} \sigma^n. \quad (64)$$

The coefficients $\lambda^{(n)}$ can be found from the operators $T^{(0)}$, $T^{(1)}$ and $T^{(2)}$ and the convergence radius can be proved to be always positive.

Before introducing the formulas with which we can calculate $\lambda^{(n)}$, we need to define some relevant operators that are derived from the unperturbed operator $T^{(0)}$. For the eigenvalue λ_0 and the eigenspace $\{e_0\}$, consider the following operators:

1. The projection P onto the subspace spanned by e_0 :

$$Pu = (u, e_0)e_0. \quad (65)$$

2. The reduced resolvent S is expressed in terms of the basis $\{e_0, e_1, e_2, \dots\}$ as

$$Su = \sum_{i=1}^{\infty} (\lambda_i - \lambda_0)^{-1} (u, e_i) e_i. \quad (66)$$

S can be thought as an inverse of $T^{(0)} - \lambda_0 I$ on the orthogonal complement of the eigenspace $\{e_0\}$. Indeed, we can make this a little more specific. Let $\tilde{T}^{(0)}$ and \tilde{S} be the restrictions of operators $T^{(0)}$ and S to the invariant subspace $(I - P_0)H$ (i.e. the orthogonal complement of the eigenspace $\{e_0\}$) respectively, then

$$\tilde{S} = (\tilde{T}^{(0)} - \lambda I)^{-1}. \quad (67)$$

It is interesting to observe that P and S completely represent $T^{(0)}$ in the perturbation method. The advantage of this representation is that P and S have simple expressions in terms of the basis. The contributions to the perturbed eigenvalue are then determined by the mutual interactions between P , S , $T^{(1)}$ and $T^{(2)}$, and a formula has been neatly derived (see for example, Kato [10]) to represent such interactions and to enable us to calculate the coefficients $\lambda^{(n)}$ in the expansion:

$$\lambda^{(n)} = \sum_{p=1}^n \frac{(-1)^p}{p} \sum_{v_1+\dots+v_p=n, k_1+\dots+k_p=p-1} tr[T^{(v_1)} S^{(k_1)} \dots T^{(v_p)} S^{(k_p)}], \quad (68)$$

where $S^{(k)} = S^k$ for integer $k > 0$, $S^{(0)} = -P$, and the symbol tr stands for the trace of a linear operator which can be defined for any operator with finite rank, as is the case here. Notice that in this formula the sum should be taken over all combinations of positive integers p with $1 \leq p \leq n$ and v_1, v_2, \dots, v_p with $v_j = 1$ or 2 , $v_1 + \dots + v_p = n$ and $k_1 + \dots + k_p = p - 1$. Although, (68) appears complicated, it is nevertheless the most efficient way to represent $\lambda^{(n)}$. Besides, a procedure can be developed to write up all the terms in (68) and this is done in the next section.

A.2 The derivation of the formulas used in perturbation method

In Kato [10], the terms in (68) up to $\lambda^{(4)}$ have been explicitly given as

$$\begin{aligned} \lambda^{(1)} &= tr[T^{(1)}P], \\ \lambda^{(2)} &= tr[T^{(2)}P - T^{(1)}ST^{(1)}P], \\ \lambda^{(3)} &= tr[-T^{(1)}ST^{(2)}P - T^{(2)}ST^{(1)}P + T^{(1)}ST^{(1)}ST^{(1)}P - T^{(1)}S^2T^{(1)}PT^{(1)}P], \\ \lambda^{(4)} &= tr[-T^{(2)}ST^{(2)}P + T^{(1)}ST^{(1)}ST^{(2)}P + T^{(1)}ST^{(2)}ST^{(1)}P \end{aligned}$$

$$\begin{aligned}
& + T^{(2)}ST^{(1)}ST^{(1)}P - T^{(1)}S^2T^{(1)}PT^{(2)}P - T^{(1)}S^2T^{(2)}PT^{(1)}P \\
& - T^{(2)}S^2T^{(1)}PT^{(1)}P - T^{(1)}ST^{(1)}ST^{(1)}ST^{(1)}P + T^{(1)}S^2T^{(1)}ST^{(1)}PT^{(1)}P \\
& + T^{(1)}ST^{(1)}S^2T^{(1)}PT^{(1)}P + T^{(1)}S^2T^{(1)}PT^{(1)}ST^{(1)}P \\
& - T^{(1)}S^3T^{(1)}PT^{(1)}PT^{(1)}P].
\end{aligned} \tag{69}$$

These formulas are essential in the perturbation method. One may find similar formulas for high order $\lambda^{(n)}$.

The next step is to evaluate the trace of the operators in the formulas obtained. This can be carried out with following formula

$$trAP = (APe_0, e_0) = (Ae_0, e_0), \tag{70}$$

which is valid for any linear operator A . Applying (70) to (69), one obtains

$$\lambda^{(1)} = (T^{(1)}e_0, e_0). \tag{71}$$

By using the explicit expression of the operator S (66) whenever applicable, one obtains:

$$\begin{aligned}
\lambda^{(2)} & = (T^{(2)}e_0, e_0) - (T^{(1)}ST^{(1)}e_0, e_0) \\
& = (T^{(2)}e_0, e_0) - \sum_i \frac{(T^{(1)}e_0, e_i)(T^{(1)}e_i, e_0)}{(\lambda_i - \lambda_0)},
\end{aligned} \tag{72}$$

where, $\sum_i = \sum_{i=1}^{\infty}$ and in all the following, we adopt the same notation. It is found that all other $\lambda^{(n)}$ can be derived in a similar way. $\lambda^{(3)}$ appears as

$$\begin{aligned}
\lambda^{(3)} & = - \sum_i \frac{(T^{(2)}e_0, e_i)(T^{(1)}e_i, e_0)}{(\lambda_i - \lambda_0)} - \sum_i \frac{(T^{(1)}e_0, e_i)(T^{(2)}e_i, e_0)}{(\lambda_i - \lambda_0)} \\
& + \sum_{i,j} \frac{(T^{(1)}e_0, e_i)(T^{(1)}e_i, e_j)(T^{(1)}e_j, e_0)}{(\lambda_i - \lambda_0)(\lambda_j - \lambda_0)} - \sum_i \frac{(T^{(1)}e_0, e_0)(T^{(1)}e_0, e_i)(T^{(1)}e_i, e_0)}{(\lambda_i - \lambda_0)^2}.
\end{aligned} \tag{73}$$

One may easily find a similar but much lengthy formula for $\lambda^{(4)}$ from (69).

B Evaluation of $I_1(m, n)$ and $I_2(m, n)$

- Evaluation of $I_1(m, n)$

$$\begin{aligned}
I_1(m, n) & = \int_0^L \sqrt{\frac{2}{L}} \sin\left(\frac{(2n-1)\pi x}{2L}\right) \left(\int_0^x \sqrt{\frac{2}{L}} \sin\left(\frac{(2m-1)\pi x}{2L}\right) dx \right) dx \\
& = \int_0^L \frac{4}{(2m-1)\pi} [1 - \cos\left(\frac{(2m-1)\pi x}{2L}\right)] \sin\left(\frac{(2n-1)\pi x}{2L}\right) dx.
\end{aligned} \tag{74}$$

By using the simple trigonometric relation $\sin(\alpha)\cos(\beta) = \frac{1}{2}\sin(\alpha + \beta) + \frac{1}{2}\sin(\alpha - \beta)$, one finds

$$I_1(m, n) = \int_0^L \frac{4}{(2m-1)\pi} \left[\sin\left(\frac{(2n-1)\pi x}{2L}\right) - \frac{1}{2}\sin\left(\frac{(n+m-1)\pi x}{L}\right) - \frac{1}{2}\sin\left(\frac{(n-m)\pi x}{L}\right) \right] dx, \quad (75)$$

which can be integrated as

$$I_1(m, n) = \begin{cases} \frac{8L}{(2m-1)^2\pi^2} & \text{if } n = m, \\ \frac{4L}{(2m-1)\pi^2} \left[\frac{4}{(2n-1)} + \frac{(-1)^{(n+m-1)-1}}{(n+m-1)} + \frac{(-1)^{(n-m)-1}}{(n-m)} \right] & \text{if } n \neq m, \end{cases} \quad (76)$$

• **Evaluation of $I_2(m, n)$**

Similarly,

$$\begin{aligned} I_2(m, n) &= \int_0^L \sqrt{\frac{2}{L}} \sin\left(\frac{(2n-1)\pi x}{2L}\right) \left(\int_0^x dx \int_0^x \sqrt{\frac{2}{L}} \sin\left(\frac{(2m-1)\pi x}{2L}\right) dx \right) dx \\ &= - \int_0^L \frac{4}{(2m-1)\pi} \sin\left(\frac{(2n-1)\pi x}{2L}\right) \left[\frac{2L}{(2m-1)\pi} \sin\left(\frac{(2m-1)\pi x}{2L}\right) - x \right] dx. \end{aligned} \quad (78)$$

By using the trigonometric relation $\sin(\alpha)\sin(\beta) = \frac{1}{2}\cos(\alpha - \beta) - \frac{1}{2}\cos(\alpha + \beta)$, one obtains

$$\begin{aligned} I_2(m, n) &= \int_0^L \frac{4L}{(2m-1)^2\pi^2} \left[-\cos\left(\frac{(m-n)\pi x}{L}\right) + \cos\left(\frac{(m+n-1)\pi x}{L}\right) \right. \\ &\quad \left. + \frac{(2m-1)\pi}{L} x \sin\left(\frac{(2n-1)\pi x}{2L}\right) \right] dx, \end{aligned} \quad (79)$$

which leads to

$$I_2(m, n) = \begin{cases} \frac{4L^2}{\pi^3} \left[\frac{-\pi}{(2m-1)^2} + \frac{4(-1)^{m+1}}{(2m-1)^3} \right] & \text{if } n = m, \\ \frac{(-1)^{n+1} 16L^2}{(2n-1)^2(2m-1)\pi^3} & \text{if } n \neq m. \end{cases} \quad (80)$$

Acknowledgment

This research was carried out with the support of Auckland University under grant No. 3606871/9344.

References

- [1] Lord Rayleigh, "On the dynamics of revolving fluids", *Proc. R. Soc. London Ser. A* **93**, **148**, (1916).
- [2] S. Wang and Z. Rusak, "The dynamics of a swirling flow in a pipe and transition to axisymmetric vortex breakdown", *J. Fluid Mech.*, **340** 177-223, (1997a).
- [3] S. Wang and Z. Rusak, "On the stability of an axisymmetric rotating flow in a pipe", *Phys. Fluids*, **8** (4), (April 1996).
- [4] A. Garg and S. Leibovich, "Spectral characteristics of vortex breakdown flow fields", *Phys. Fluids*, **22** (11), (1979).
- [5] T. Mattner, P. Joubert and M. Chong, "Vortical flow. Part 1: Flow in a constant diameter pipe", *J. Fluid Mech.*, **463** 259-291, (2002).
- [6] F. Gallaire and J.-M. Chomaz, "The role of boundary conditions in a simple model of incipient vortex breakdown", *Phys. Fluids*, **16** (2), (February 2004).
- [7] A. Szeri and P. Holmes, "Nonlinear stability of axisymmetric swirling flows", *Philos. Trans. R. Soc. London Ser. A*, **326.**, 327, (1988).
- [8] H.B. Squire, "Rotating fluids", *Surveys in Mechanics*, edited by G. K. Batchelor and R.M. Davies (Cambridge University Press), Cambridge, 139-161, (1956)
- [9] R.R. Long, "Steady motion around a symmetrical obstacle moving along the axis of a rotating liquid", *J. Meteorol.*, **10**, 197, (1953).
- [10] T. Kato, "Perturbation Theory for Linear Operators", *Die Grundlehren der mathematischen Wissenschaften*, Springer-Verlag, New York, **vol. 132**, (1966).
- [11] F. Gallaire, J.-M. Chomaz and P. Huerre, "Closed-loop control of vortex breakdown: a model study", *J. Fluid Mech*, **511**, 67-93, (2004).